HHS Public Access

Author manuscript

Drug Deliv Transl Res. Author manuscript; available in PMC 2016 September 08.

Published in final edited form as:

Drug Deliv Transl Res. 2015 December ; 5(6): 611–624. doi:10.1007/s13346-015-0260-0.

Visible light and near infrared-responsive chromophores for drug delivery-on-demand applications

Chase S. Linsley[1], **Viola Y. Quach**[1], **Gaurav Agrawal**[1], **Elyse Hartnett**[1], and **Benjamin M. Wu**[1,2,*]

[1]Department of Bioengineering, University of California, Los Angeles, Los Angeles, CA 90095, USA

[2]Division of Advanced Prosthodontics and the Weintraub Center for Reconstructive Biotechnology, University of California, Los Angeles, Los Angeles, CA 90095, USA

Abstract

The need for temporal-spatial control over the release of biologically active molecules has motivated efforts to engineer novel drug delivery-on-demand strategies actuated via light irradiation. Many systems, however, have been limited to *in vitro* proof-of-concept due to biocompatibility issues with the photo-responsive moieties or the light wavelength, intensity and duration. To overcome these limitations, this paper describes a light actuated drug delivery-on-demand strategy that uses visible and near infrared (NIR) light and biocompatible chromophores: cardiogreen, methylene blue and riboflavin. All 3 chromophores are capable of significant photothermal reaction upon exposure to NIR and visible light, and the amount of temperature change is dependent upon light intensity, wavelength as well as chromophore concentration. Pulsatile release of bovine serum albumin (BSA) from thermally-responsive hydrogels was achieved over 4 days. These findings have the potential to translate light actuated drug delivery-on-demand systems from the bench to clinical applications that require explicit control over the presentation of biologically active molecules.

Keywords

Triggered release; Photothermal effect; Visible light; Near-infrared light; Cardiogreen; Methylene blue; Riboflavin

Introduction

Traditional methods of drug delivery, which load the body with high concentrations of drug, have problems with drug instability, toxicity and overcoming barriers to the target area from the circulation system [1]. To overcome these drawbacks, delivery systems were developed to localize the delivery, enable rapid onset of action, reduce the amount of drug required, and

*Corresponding Author and Reprint Requests: Benjamin M. Wu, D.D.S., Ph.D., 420 Westwood Plaza, Room 5121, Engineering V. P.O. Box: 951600, Los Angeles, CA 90095-1600, Fax: (310) 794-5956, benwu@ucla.edu.

Conflict of Interest Disclosure: C. Linsley, V. Quach, G. Agrawal, E. Hartnett and B. Wu declare that they have no conflict of interest.

improve patient compliance. One approach is drug delivery-on-demand systems. These systems modulate the release of drugs as a function of stimuli intensity [1-4]. Stimuli that have been used to control release include: light irradiation, heat, electrical or magnetic fields, mechanical compression and ultrasound. Light as the stimulus for drug delivery-on-demand systems is advantageous for a number of reasons: it is non-invasive, convenient, easy to use, and offers high spatial resolution and temporal control.

Many light actuated systems use ultraviolet (UV) light to act upon photo-responsive moieties within the polymeric drug delivery vehicles. The photo-responsive moieties use UV light for either isomerization or chemical reactions that facilitate release [5]. However, the reliance on UV radiation hinders clinical translation due to low tissue transparency in the UV region [6]. Additionally, repetitive low-dose (18 J/cm^2) exposure to UVA radiation (320-400nm) caused an increase in inflammatory infiltrates, depleted Langerhans cells and increased lysozyme deposition in human skin [7]. Furthermore, photo-responsive moieties (e.g. azobenzene) and some of their degradation products are considered toxic by the U.S. Food and Drug Administration (FDA) [1, 8]. For these reasons, light actuated drug delivery-on-demand systems currently serve as proof-of-concept models only due to the problems with mutagenicity, toxicity and biocompatibility. Despite these shortcomings, light actuated drug delivery-on-demand systems offer precise and explicit triggering of release as well as versatility in clinical applications. Therefore, the development of a light actuated system that improves upon the shortcomings of UV systems will advance the clinical applications of light actuated drug delivery-on-demand systems.

Visible and near infrared (NIR) light actuation eliminates the negative side effects that accompany UV irradiation, such as DNA and tissue damage [6, 9], thereby making them a safe stimulus for *in vivo* applications. Furthermore, utilizing non-toxic and biocompatible chromophores for visible and NIR light eliminates the need for toxic photo-responsive materials. In this approach, the radiationless dissipation of a chromophore's excess energy from an absorbed photon can serve as a heat source, and this photothermal effect can be used to release biologically active molecules from a thermally responsive polymeric delivery vehicle.

This study aimed to characterize the photothermal effect of cardiogreen, methylene blue and riboflavin upon light irradiation, and demonstrate triggered release. Cardiogreen, methylene blue and riboflavin are non-toxic and biocompatible, unlike azobenzene and o-nitrobenzene used in UV systems. Cardiogreen has multiple medical diagnostic applications, such as measuring cardiac output [10]. Methylene blue is used in technologies that sterilize blood products through photo-inactivation [11, 12], and riboflavin is naturally occurring in the body as a constituent of the coenzymes flavin mononucleotide and flavin adenine dinucleotide [13]. Additionally, these chromophores have absorption peaks in the NIR or visible region. Cardiogreen has a NIR absorbance peak at 780 nm [10], and methylene blue absorbs in the red region with a major peak at 665 nm [12]. The absorption spectrum of riboflavin shows four distinct absorbance peaks with one of the peaks in the visible region at 445 nm [14]. Furthermore, the quantum efficiency of fluorescence for these chromophores is low, which suggests there is a high occurrence of radiationless transitions – one of which is heat generation – when these molecules are excited with light. Cardiogreen's quantum

efficiency for fluorescence is 0.027 in water [10]. Methylene blue has a quantum efficiency of 0.01 in aqueous solutions [15], and the quantum efficiency of riboflavin is 0.26 at neutral pH in an aqueous solution [14]. By selecting these biocompatible chromophores, biologically active molecules can be photothermally released on-demand from thermally responsive delivery vehicles.

Materials and Methods

Chromophores

Riboflavin was purchased from Acros Organics (CAS number 83-88-5; New Jersey, USA). Methylene blue was purchased from Thermo Fisher Scientific (CAS number 61-73-4; Massachusetts, USA). Cardiogreen was purchased from Sigma-Aldrich (CAS number 3599-32-4; Missouri, USA). Their absorption spectra and chemical structure are shown in Fig. 1. All chromophores were used without further purification.

Chromophore-dependent temperature change

Aqueous solutions of each chromophore were prepared by dissolving the chromophores in deionized water. The final concentrations were 0.1, 0.05, and 0.01 mg/mL for cardiogreen, methylene blue and riboflavin. To measure the photothermal effect for each chromophore, 1 mL solutions of each chromophore were added to disposable cuvettes that were optically transparent for visible and NIR light (Fig. 2a). The final molar concentrations were 12.9, 64.5, and 129 μM for cardiogreen; 31.3, 156, and 313 μM for methylene blue; and 26.6, 133 and 266 μM for riboflavin.

Wavelength- and power-dependent temperature change measurements were achieved by irradiating with a POLILIGHT® PL500 multi-wavelength light source (Rofin, Australia). The central wavelengths and corresponding bandwidths are listed in Supplement Table 1. A Fluke 54 Series II thermometer (Fluke Corporation, Washington, USA) was used to record rate of temperature change as well as the final temperature change after irradiation for all experiments. For power-dependent temperature change, the chromophore solutions at varying concentrations were irradiated by visible or NIR light at varying power intensities (100, 300, and 500mW) for 5 min. The light intensity used for each chromophore's wavelength-dependent temperature change was 600mW and the light intensities for the rate of temperature change were 600mW and 750mW. The experiments were conducted in triplicate and the average values are represented with the standard error.

Photothermal-triggered release from thermally responsive NiPAAm

Poly (N-isopropylacrylamide) (NiPAAm) (CAS number 25189-55-3, Sigma-Aldrich, Missouri, USA) hydrogels were fabricated using the procedure previously described by Zhang, et al [16]. Briefly, NiPAAm was dissolved in 50:50 water and acetone solution along with the crosslinker N, N′-methylenebisacrylamide (MBA) (CAS number 110-26-9, Sigma-Aldrich, Missouri, USA). This mixture was polymerized with N, N, N′, N′-tetramethylethylenediamine (TEMED) (CAS number 110-18-9, Acros Organics, New Jersey, USA) and 10% (w/v) ammonium persulfate (APS) (CAS number 7727-54-0, Sigma-

Aldrich, Missouri, USA), and then soaked and stirred in deionized water (dH_2O) for at least 24 h to leach away unreacted products.

Bovine serum albumin (BSA) (Fisher Scientific, New Jersey, USA) was used as a model drug (66 kDa) for triggered release. To load BSA, the NiPAAm hydrogels were incubated in a 60°C water bath for 10 min to de-swell and then transferred to a 1% (w/v) BSA solution to soak at 4°C for 24 h.

Cardiogreen was loaded into the NiPAAm hydrogel via electrophoresis (Fig. 2b). Briefly, two wells were separated by an impermeable divider that included the NiPAAm hydrogel. 10 mL of phosphate buffered saline (PBS, Thermo Fisher Scientific, Massachusetts, USA) solution was added to the well with the positive lead and 10 mL of the cardiogreen solution was added to the well with the negative lead. For control hydrogels, which contained no cardiogreen, tap water was used in place of the cardiogreen solution. A MicroJet III Controller (MicroFab, Technologies, Inc., Texas, USA) was used to supply 140 V for 5 min and electrostatically load cardiogreen into the NiPAAm hydrogel (Supplement Fig. 1). The resulting hydrogel had a cardiogreen gradient, and the surface exposed to the cardiogreen solution during electrophoresis loading was the same surface that later received near infrared light irradiation during the triggered release studies.

In order to measure the release of BSA from the NiPAAm hydrogels, a modified conical tube and petri dish setup was designed (Fig. 2c). Briefly, the NiPAAm hydrogel was placed at the mouth of a 15mL conical tube body to ensure the same surface was exposed to the supernatant for the duration of the experiment. The exposed surface of the NiPAAm hydrogel was submerged in 10 mL of dH_2O in a transparent petri dish, and to prevent the opposite face of the hydrogel from dehydration during the course of the experiment, parafilm was used to seal the top of the conical tube while capillary action kept the hydrogel hydrated. The conical tube body was held up by a modified petri dish cover and secured by rubber O-rings. The NIR light source was positioned below the setup. During the experiment, 1 mL samples of the supernatant were collected from the petri dish at designated time points. Specifically, at times 0, 1 and 60 min on day 1 and every 24 h thereafter for 2 weeks. To keep the supernatant volume constant at 10 mL, 1 mL of fresh dH_2O was added to replace the volume taken at each time point.

For samples exposed to NIR light, the supernatant solution was heated to 27°C immediately prior to irradiation. This temperature is 5°C below the lower critical solution temperature of NiPAAm. Starting at the 24 h time point, the NiPAAm hydrogels were irradiated with NIR light at 750mW or 1.2W for 1-2 min. The 1 mL supernatant sample was collected 5 min after light irradiation started. This process was repeated every 24 h for 4 days.

The amount of BSA released at each time point was determined by using the BCA assay (Pierce, Thermo Scientific, Illinois, USA). Following the assay manufacturer's protocol, the absorbance was read on an Infinite F200 plate reader (Tecan, Männedorf, Switzerland). The experiments were conducted in two sets of duplicates for each experimental group and the average values are represented with the standard error.

Results

Concentration- and power-dependent temperature changes

Aqueous solutions of cardiogreen, methylene blue and riboflavin were exposed to 3 power intensities (100mW, 300mW, and 500mW) of light that corresponded with the absorption peak of each chromophore. In addition, the effect of chromophore concentration (0mg/mL to 0.1mg/mL) on total temperature change was examined. The data shows that with increasing chromophore concentration and increasing light intensity there is an increase in the temperature rise. In all cases, the presence of a chromophore results in a greater temperature change when compared to water with no added chromophore (Fig. 3).

Cardiogreen—The final temperature change of an aqueous solution of cardiogreen at 0.1mg/mL after exposure to 500mW of NIR light was 6.9°C (±0.2°C), whereas a 0.01mg/mL solution of cardiogreen at the same power intensity produced a final temperature change of 5.2°C (±0.1°C). Similar temperature changes were achieved when 0.05mg/mL and 0.1mg/mL solutions of cardiogreen were irradiated with 300mW (6.2°C (±0.3°C) and 6.3°C (±0.4°C), respectively). For all the solutions irradiated with 100mW of NIR light the change in temperature measured was less than 2°C. The greatest temperature change in samples of water with no chromophore added was 3°C at 300mW and 500mW (Fig. 3a).

Methylene Blue—After exposure to 500mW of 650nm light, the final temperature change of an aqueous solution of methylene blue at 0.1mg/mL was 5.9°C (±0.3°C), and a 0.01mg/mL solution of methylene blue at the same power intensity produced a final temperature change of 5.5°C (±0.1°C) (Fig. 3b). At each power intensity there is a similar temperature change achieved between the various concentrations of methylene blue solutions. For instance, methylene blue solutions irradiated with 300mW had temperature changes ranging between 3.5°C to 4°C. Additionally, for all the solutions irradiated with 100mW of 650nm light the change in temperature measured was less than 2°C. This was greater than the temperature change caused by water with no chromophore added which increased in temperature by less than 1.5°C even at 500mW.

Riboflavin—The final temperature change of an aqueous solution of riboflavin at 0.1mg/mL after exposure to 500mW of 450nm light was 7.4°C (±0.1°C), whereas a 0.01mg/mL solution of riboflavin at the same power intensity produced a final temperature change of 2.1°C (±0.3°C) (Fig. 3c). A similar temperature change was achieved when 0.01mg/mL solutions of riboflavin were irradiated with 300mW (1.9°C (±0.1°C)). For all the solutions irradiated with 100mW of 450nm light the change in temperature measured was less than 2°C. However, this was still greater than the temperature change caused by water with no chromophore added which increased in temperature by less than 1°C even at 500mW.

Wavelength-dependent temperature change

As seen in Fig. 1, each chromophore has an absorption peak either in the visible or NIR light region of the spectrum with cardiogreen's absorption peak in the NIR region between 780-900 nm, methylene blue's in between 580-680nm, and riboflavin's appearing in the blue

region (400-500 nm). The greatest temperature change is observed near the absorption maxima while wavelength outside the absorption bands produce smaller temperature changes (Fig. 4).

Cardiogreen—The absorption maximum for cardiogreen is 780 nm. Exposure to 600mW of NIR light demonstrated a concentration dependent temperature change below 0.05mg/mL: 9.9°C (±0.4°C) (0.1mg/mL); 9.8°C (±0.2°C) (0.05mg/mL); and 7.7°C (±0.1°C) (0.01mg/mL). Outside the absorption band, the higher cocentrations have a significant temperature change over water alone but less than the temperature change in the NIR region. Between 490 nm and 555 nm the change in temperature ranges from: 3.5°C (0.05mg/mL) to 5.0°C (0.1mg/mL). Cardiogreen has a second smaller peak between 400 nm and 500 nm. The tempature change in this region demonstrated concentration dependent temperature changes and ranged from 7.4°C (±0.1°C) (0.1mg/mL; 415nm) to 2.0°C (±0.1°C) (0.01mg/mL; 470nm). This is greater than the temperature change measured outside the abosption peaks but less than the larger abosprtion peak in the NIR region (Fig. 4a).

Methylene blue—The absorption maximum for methylene blue is 665 nm. Exposure to 650 nm light (600mW) caused significant temperature changes at all concentrations: 11.4°C (±0.2°C) (0.1mg/mL); 11.2°C (±0.2°C) (0.05mg/mL); and 9.9°C (±0.2°C) (0.01mg/mL). Outside the absorption band, methylene blue demonstrates a significant temperature change over blank water samples, different from riboflavin but similar to cardiogreen. For example, at 415 nm (600mW) the measured temperature change was 4.6°C (±0.4°C) (0.1 mg/mL). The lowest concentration shown (0.01 mg/mL), however, follows a similar pattern where the greatest temperature change corresponds with the absoprtion max and little temperature change outside the absorption band (1.8°C (±0.2°C) at 415 nm) (Fig. 4b). Since there was little difference in the measured temperature changes within the absorption band between the three concentrations of methylene blue, the concentration was lowered to evaluate how low the concentration of methylene blue could be and still have a meaningful temperature change over water. Two additional concentrations were measured, 0.005mg/mL and 0.001mg/mL. 0.001mg/mL had a temperature change of 3.8°C (±0.1°C) at 650 nm (600mW), nearly 2°C more than water under the same conditions (Fig. 4c). At 590 nm (600mW), the difference had decreased to 0.5°C with methylene blue at 2.6°C (±0.1°C) and water at 2.1°C (±0.2°C) (Fig. 4c).

Riboflavin—The absorption maximum for riboflavin is 445 nm. Exposure to 415 nm light (600mW) demonstrated a concentration dependent temperature change: 9.9°C (±0.1°C) (0.1 mg/mL); 8.1°C (±0.2°C) (0.05mg/mL); and 3.4°C (±0.3°C) (0.01mg/mL). Outside the absorption band, very little temperature change is measured starting at 530 nm where there is no difference between the different concentrations: 2.2°C (±0.1°C) (0.1mg/mL); 1.6°C (±0.1°C) (0.05mg/mL); and 1.7°C (±0.2°C) (0.01mg/mL) (Fig. 4d).

Chromophore lifetime

To study each chromophore's lifetime for heat generation, cardiogreen, methylene blue and riboflavin underwent 5 minute exposures every 24 h for 7 days to 600mW of NIR or visible light, corresponding with each chromophore's absorption max. The data shows that

cardiogreen and methylene blue had no loss in their photothermal abilities between time points and showed a prolonged lifetime for heat generation while riboflavin had a steady decrease in heat generation over the 7 days. The temperature change of 1 mL aqueous solutions loaded with 0.1mg/mL of cardiogreen ranged between 9.9°C and 12.6°C (Fig. 5a), and the methylene blue solutions had temperature changes that ranged between 7.1°C and 8.3°C (Fig. 5b). The riboflavin solutions had a 7°C (±0.2°C) change in temperature at day 1 that decreased to 2.5°C (±0.1°C) by day 7. Decreasing the power of light to 500mW helped to prolong the lifetime for heat generation; however, at day 5 the temperature change caused by irradiating riboflavin with blue light dropped to 5.5°C (±0.1°C) and was down to 3.6°C (±0.1°C) at day 7 (Fig. 5c).

3.4 Rate of chromophore-dependent temperature change

Fig. 6 shows the rate of heat generation by cardiogreen, methylene blue and riboflavin (0.1mg/mL) upon irradiation with NIR or visible light. The temperature change of cardiogreen after 1 minute of NIR light exposure was 2.5°C (±0.2°C) and 4.4°C (±0.3°C) after 2 min of exposure at 600mW with an average temperature change rate of 2.2°C/min. For methylene blue, after 1 minute of exposure to 650 nm light, the temperature change was 2.7°C (±0.1°C) and 4.4°C (±0.1°C) after 2 min of exposure at 600mW with an average temperature change rate of 2.2°C/min. Riboflavin generated 3.3°C (±0.1°C) of heat at 1 minute and 5.6°C (±0.1°C) after 2 min of exposure to 450 nm light at 600mW with an average temperature change rate of 2.8°C/min (Fig. 6a).

The advantage of NIR light over visible light is the limited light attenuation in tissues. However, water also absorbs NIR light more strongly. For *in vivo* applications, rapid temperature change over water is necessary for chromophore-dependent heat generation. The temperature change of cardiogreen after 1 minute of NIR light exposure at 750mW was 5.4°C (±0.1°C) and 9.4°C (±0.1°C) after 2 min of exposure with an average temperature change rate of 4.7°C/min. For methylene blue, after 1 minute of exposure to NIR light, the temperature change was 3.7°C (±0.1°C) and 6.0°C (±0.1°C) after 2 min of exposure at 750mW with an average temperature change rate of 3.0°C/min. Riboflavin generated 3.2°C (±0.1°C) of heat at 1 minute and 5.0°C (±0.1°C) after 2 min of exposure to NIR light at 750mW with an average temperature change rate of 2.5°C/min, however this heat generation was due to water absorbing the NIR light (Fig. 6b).

Due to cardiogreen's robust photothermal response upon irradiation with NIR light, it was selected for the triggered release studies. To confirm loading cardiogreen into NiPAAm hydrogels did not impact cardiogreen's photothermal response, the temperature change rate upon irradiation was measured. After 1 minute of NIR light exposure at 750mW, the temperature change was 5.6°C and 9.6°C after 2 min of exposure with an average temperature change rate of 4.8°C/min (Fig. 6c).

Photothermal-triggered release from thermally responsive NiPAAm

NiPAAm is a well known temperature-sensitive hydrogel and exhibits a lower critical solution temperature (LCST) around 32°C. As the temperature increases it becomes hydrophobic and expels water molecules, including the payload molecules, as it goes from a

hydrogel to a globular structure. NiPAAm hydrogels were loaded with BSA and the release profile over four days was determined. Any protein absorbed to the surrounding surface was considered to be negligible.

Fig. 7a compares the release profiles of BSA due to diffusion and light actuation. All samples show an initial burst release within the first 24 h – 43μg (±2μg) from the diffusion samples, 41μg (±5μg) from NIR light samples without cardiogreen, and 53μg (±4μg) from NIR light samples with cardiogreen. The first light exposure (1 minute at 750mW) triggered the release of 49μg of BSA from the hydrogels loaded with cardiogreen compared to 27μg from the NiPAAm hydrogels alone. The second, third and fourth exposure triggered the release of 50μg, 42μg and 47μg of BSA from the hydrogels loaded with cardiogreen and 32μg, 37μg and 44μg from the hydrogels alone, respectively. In total, 319μg (±9μg) of BSA was released after 4 days by the photothermal effect of cardiogreen acting upon the NiPAAm hydrogel compared to 223μg (±5μg) and 121μg (±7μg) of BSA from NIR light irradiation without cardiogreen and diffusion only, respectively.

The effect that increasing the light power from 750mW to 1200mW has on the release of BSA from NiPAAm hydrogels is seen in Fig. 7b. Similar burst release within the first 24 h due to diffusion is seen (46μg (±2μg)). The first light exposure triggered the release of 55μg (±8μg). The second, third and fourth exposure triggered the release of 40μg (±2μg), 41μg (±4μg) and 49μg (±6μg), respecitively. In total, 274μg (±27μg) of BSA was released from NiPAAm hydrogels loaded with cardiogreen and irradiated with 1200mW of NIR light for 1 minute.

The effect that increasing the exposure time to 750mW of NIR light from 1 minute to 2 min has on the release of BSA from NiPAAm hydrogels is seen in Fig. 7c. Again, there is an initial burst release within the first 24 h due to diffusion (69μg (±12μg)). The first light exposure triggered the release of 69μg (±8μg) of BSA. The second, third and fourth exposure triggered the release of 56μg (±4μg), 36μg (±4μg) and 36μg (±2μg), respecitively. In total, 288μg (±24μg) of BSA was released from NiPAAm hydrogels loaded with cardiogreen and irradiated with 750mW of NIR light for 2 min.

To determine the percent of BSA released from the NiPAAm hydrogels, the mass released at each timpoint,M_t, was divided by the mass released at time infinity, M_∞. A preliminary study of the BSA release profile from NiPAAm hydrogels due to diffusion over 28 days showed a plateau in release by day 14 (data not shown). Therefore, M_∞ was set at day 14 (Fig. 7d). After 4 days of 4×1 minute NIR light exposures at 750mW, 80% of the BSA had been released from the NiPAAm hydrogel. 13% of the loaded BSA is released from the initial burst release. The first light exposure triggers the release of 12% of the BSA. The second, third and fourth exposures trigger 12%, 11% and 12% of the BSA to release, respectively.

Discussion

The choice of cardiogreen, methylene blue and riboflavin as chromophores for drug delivery-on-demand applications via NIR and visible light actuation highlights the novelty

of this study. The current biomedical application for riboflavin is to act as a type II photo-initiator for hydrogel polymerization reactions which uses riboflavin's absorption in the visible region as a safe alternative to using harmful UV irradiation [17, 18]. Methylene blue is actively researched for photo-inactivation technologies in European countries. Viruses, including Hepatitis B, Hepatitis C, HIV, B19 virus and West Nile virus, have been inactivated in fresh blood plasma with 1μM methylene blue and visible light exposure [11, 12, 19]. Finally, cardiogreen is the only FDA approved NIR dye for medical diagnosis [20]. Specifically, cardiogreen is clinically used to evaluate blood flow and liver function (i.e. clearance) [21, 22] although there is growing interest in using cardiogreen for tumor ablation [23]. Advancing the biomedical application of these chromophores, this study 1) characterized and identified the optimal photothermal response of these materials for drug delivery-on-demand applications; and 2) in the case of cardiogreen, demonstrated triggered release of BSA from the thermally responsive delivery vehicle, NiPAAm. Specifically, this study achieved 5°C temperature change rapidly (<2 min). Necessary since 5°C above physiological temperature (37°C) is the threshold for tissue damage from hyperthermia and prolonged light irradiation can lead to high temperatures that cause tissue ablation within seconds as well as raise the temperature of surrounding tissue via thermal conduction [24, 25]. Additionally, the rapid photothermal response of the chromophores, specifically cardiogreen, is necessary to outpace the heating due to absorption of NIR light by water which has a low absorption coefficient, but non-negligible, between 700-900nm [26, 27]. The key properties and photothermal results for the chromophores are summarized in Table 1. These conditions were used to uniformly trigger the release of BSA over 4 days from a rapidly responding NiPAAm hydrogel – prepared using a mixed solvent for the polymerization reaction that produced an expanded hydrogel structure that exhibits a rapid, thermodynamically driven phase transition [16].

The *in vivo* application and microenvironment determine the delivery-on-demand systems operating parameters. Specifically, light attenuation in biological tissues due to absorption by chromophores like hemoglobin and scattering by collagen fibers [9] limits the intensity of light in deeper tissues (Supplement Fig. 2), and according to the inverse-square law, light intensity is proportional to the inverse square of the distance from the light source [28]. Consider the blue (400-500nm) region of light. All three chromophores induce a significant change in temperature over water in this region (riboflavin and cardiogreen have absorption peaks in this region and methylene blue demonstrates a blue shift in absorption due to dimerization at high concentrations [29]). However, these wavelengths are strongly absorbed by hemoglobin and penetration depth into the body is limited to a few microns so clinical applications are limited to surfaces. Additionally, visible light has been shown to have a dose-dependent increase in reactive oxygen species generation in the range of solar irradiance [30] and the light intensities used for this study are greater than ambient light. Since the results show that each chromophore has a dose-dependent and power-dependent temperature change, these variables can be customized to fit the requirements of each potential application. This is also true for the wavelength of light and for example, applications requiring greater tissue penetration can select methylene blue or cardiogreen which produce significant temperature changes in the red and NIR regions of light, respectively. Finally, the pH of the environment needs to be considered since it impacts the

efficiency in which light energy is converted into thermal energy (Supplement Fig. 3). Therefore, light power, time of exposure, pH and wavelength are all variables that need to be considered when designing light actuated drug delivery-on-demand systems for future clinical applications.

The lifetime for the photothermal response of the chromophores studied varied and is dependent upon the photostability of each chromophore. This is because absorbed light causes electron excitation that can result in radical formation in the excited singlet and triplet states. Radicals are highly reactive species that can disrupt the conjugated double bonds responsible for the absorption of NIR or visible light. The prolonged photothermal response of cardiogreen seen in this study is due to the low quantum yield for triplet formation, which previous studies looking at the photostability of cardiogreen report in water and human plasma is 2.2×10^{-3} and 0.026, respectively [31]. Additionally, cardiogreen forms J-aggregates at higher concentrations (similar to the concentration used in this study) which protect it from conformational changes that lead to radical formation and subsequent degradation that occurs at lower concentrations [31, 32]. Similarly, methylene blue forms dimers at higher concentrations that help stabilize the molecules, which has a high quantum yield for triplet formation at low concentrations (0.52) [33]. Riboflavin also has a high quantum yield for triplet formation (0.6) [34]. Unlike cardiogreen and methylene blue, however, riboflavin undergoes photobleaching and is no longer sensitive to light. The main products from the photolysis of riboflavin are lumichrome and lumiflavin and are obtained by the oxidation of the ribityl side-chain [35]. Previous work has used citrate buffer to stabilize riboflavin against photolysis [36] and may have utility in drug delivery-on-demand applications by stabilizing the photothermal response of chromophores for long-term use, including cardiogreen and methylene blue, which may be less stable at lower concentrations.

Because these molecules have the potential to produce reactive oxygen species such as singlet oxygen or free radicals upon light irradiation, they can be toxic to cells and lead to irreversible damage [37]. For instance, previous studies looking at the reactive oxygen species generation of cardiogreen found that when irradiated with $2W/cm^2$ 808 nm laser for 5 min, the amount of reactive oxygen species was higher than the positive control of H_2O_2 and 3.4 times higher than the negative control [37]. Additionally, it was seen that increased riboflavin concentration and visible light exposure resulted in decreased cell viability [38]. This is from the generation of hydrogen peroxide – a common product of free radical generation in aqueous solutions [39]. To combat this deleterious outcome, the human eye has been used as inspiration, where excess vitamin C (ascorbic acid) is present to act as a free radical scavenger [40]. The effect of adding 2.5mM of ascorbic acid to the system was studied, and was shown not to influence the photothermal response of the chromophore (Supplement Fig. 4). It is worth noting that for certain clinical indications it may be advantageous to allow free radical (and subsequent H_2O_2) generation to occur (known as Photodynamic Therapy (PDT) and sometimes used to treat oncological, cardiovascular, and ophthalmic diseases [41]) and couple it with drug delivery-on-demand.

Cardiogreen irradiated with NIR light was selected for the triggered release because: 1) cardiogreen's safety - low quantum yield for triplet formation and subsequent free radical production; 2) cardiogreen's rapid photothermal response upon irradiation; 3) NIR light's

greater penetration depth in tissues than visible light; and 4) cardiogreen's absorption peak in the NIR region. The results show that uniform spikes in BSA release with 1 minute of 750mW NIR light exposure every 24 h for 4 days was achieved in dH_2O. While a more physiologically relevant medium (e.g. PBS) could have been used, it is not expected to have a significant impact on the release kinetics since electrostatic interactions are not the mechanism of release as they are in affinity controlled release systems. Additionally, the lifetime for the photothermal response of cardiogreen is ≥7 days, yet only 4 days' worth of triggered release was possible. The reason for this is that cardiogreen, as well as methylene blue and riboflavin, are small molecules that can easily diffuse from the hydrogel network and decrease the concentration of chromophore over time – eventually dropping below the lower limit required for heat generation within the thermally responsive delivery vehicle. The incorporation of chromophore reservoirs (micro-particles loaded with chromophore) could alleviate this limitation by delaying the diffusion of chromophore away from the scaffold and maintaining the threshold concentration for a therapeutically relevant timeline. Alternatively, these chromophores could also be chemically conjugated to the scaffold to prevent chromophore elution [41, 42].

The amount of BSA released during each light exposure is controlled by a *collapse region* where the pores of the collapsing network are sufficiently large enough for the displaced protein to escape the network. Traditionally, NiPAAm hydrogels have been prepared with a purely aqueous solvent that promoted the formation of a dense skin layer upon heating and hindered the permeation of both water and BSA (thereby turning ‘off’ release upon light irradiation). In this study, the NiPAAm hydrogels were fabricated using a mixed solvent to prevent skin formation [16] and produce a rapidly and uniformly deswelling hydrogel for release via squeezing [43]. Specifically, as the surface of the NiPAAm delivery vehicle is heated by the photothermal response of cardiogreen irradiated with NIR light, the network transitions from a swollen hydrogel network to a collapsed network and expels water and protein [44]. As the network continues to collapse, the pores will eventually become too small for BSA from deeper inside the hydrogel network to readily escape, thereby preventing more of the protein from being released. The size of the *collapse region* is determined by the heating depth and can be modulated by both the intensity of light and time of light exposure. However, the triggered release profiles show little difference in BSA release between the light intensities and exposure times studied. A reason for this may be that less BSA remains in the hydrogel over time. Since more heat is generated during longer light exposures and with greater light intensities, more heat is transferred further into the gel creating a larger region of the gel that collapses, which releases the water and BSA occupying the space. This decreases the concentration gradient that drives diffusion of BSA within the hydrogel itself, and prevents the same concentration of BSA from occupy the evacuated volume as before. This is demonstrated by the greater amount of BSA release seen at the first light exposure in the samples irradiated with 1200mW and both the first and second light exposures in the samples irradiated for 2 min that are then followed up by significant decreases in the amount of BSA released with subsequent light exposures. Ultimately, while uniform triggered release of BSA was achieved with 1 minute of 750mW NIR light exposure every 24 h in this study, future systems will need to consider loading

concentration and delivery vehicle dimensions in addition to time of exposure and light intensity to achieve prolonged uniform triggered release.

The delivery-on-demand results are compared with other NIR actuated systems in Table 2. Perhaps the most widely researched materials for applications actuated by NIR light are gold nanoparticles; however, gold nanoparticles are limited by issues with toxicity both *in vitro* and *in vivo*. When delivered intravenously, gold nanoparticle accumulation has been seen in liver, lung, and spleen tissue and in heart, kidney and brain tissue to a small degree [45]. A study in BALB/c mice showed that 13nm-sized gold nanoparticles induced inflammation and apoptosis in liver tissue after 7 days [46]. Recently, a NIR actuated delivery system was designed where water was confined within poly (lactic-co-glycolic acid) (PLGA) particles and released fluorescein as the water was heated above the polymer's glass transition temperature [47]. A key strength of the system is the biocompatibility since PLGA is already used in FDA-approved implantable devices; however, the system is slow to respond as it takes 5 min of light exposure to trigger release and all light cycles occurred within 90 min. In contrast, the reported system released BSA from NiPAAm within 1 minute of light exposure for 4 cycles over 4 days. Despite studies demonstrating NiPAAm's biocompatibility [48-50], there are concerns regarding the *in vivo* safety of NiPAAm due to the toxicity of the monomer [51, 52]. However, adaptation of the reported strategy for delivery-on-demand to novel biocompatible thermally responsive delivery vehicles, such as thermally responsive hydrogels based on polypeptides, may be used to overcome concerns regarding the biocompatibility and cytotoxicity of the reported delivery vehicle. One example is the block co-polymer (ethylene glycol)–(DL-alanine)–(L-alanine) whose hydrophilic-hydrophobic balance and block sequence with a flexibility gradient creates a thermo-sensitive polymer that is a hydrogel at 37°C and a squeezed gel above 40°C [53], and in addition to being biocompatible, is also biodegradable via enzymatic degradation. [54] Ultimately, further research into the design and fabrication of novel biocompatible thermally responsive delivery vehicles will aid in the advancement of the light actuated drug delivery-on-demand approach described here.

Conclusion

In this proof-of-concept study, a new strategy for triggered release via near infrared light (NIR) actuation for future biomedical applications is described. The data demonstrates the feasibility of and parameters for using irradiated riboflavin and methylene blue as actuators for the controlled delivery of biologically active molecules and demonstrates triggered release of protein from a thermally responsive delivery vehicle loaded with cardiogreen and irradiated with NIR light. Specifically, it was shown that each of these chromophores is capable of significantly increasing the temperature of aqueous solutions upon exposure to visible or NIR light. The amount of temperature change is dependent upon light intensity, wavelength, as well as chromophore concentration. Finally, the rapid release of BSA upon NIR light exposure from NiPAAm was achieved over 4 cycles with 24 h between light exposures. The amount of BSA released showed little dependence on the amount of light exposure time and light intensity for the conditions studied. Ultimately, this drug delivery strategy has potential for clinical applications that require explicit control over the presentation of biologically active molecules.

Supplementary Material

Refer to Web version on PubMed Central for supplementary material.

References

1. Alvarez-Lorenzo C, Bromberg L, Concheiro A. Light-sensitive Intelligent Drug Delivery Systems. Photochemistry and Photobiology. 2009; 85(4):848–60. [PubMed: 19222790]
2. LaVan DA, McGuire T, Langer R. Small-scale systems for in vivo drug delivery. Nature Biotechnology. 2003; 21(10):1184–91.
3. Kost J, Langer R. Responsive polymeric delivery systems. Advanced Drug Delivery Reviews. 2001; 46(1-3):125–48. [PubMed: 11259837]
4. Sershen S, West J. Implantable, polymeric systems for modulated drug delivery. Advanced Drug Delivery Reviews. 2002; 54(9):1225–35. [PubMed: 12393303]
5. Tomatsu I, Peng K, Kros A. Photoresponsive hydrogels for biomedical applications. Advanced Drug Delivery Reviews. 2011; 63(14-15):1257–66. [PubMed: 21745509]
6. Tadokoro T, Kobayashi N, Zmudzka BZ, Ito S, Wakamatsu K, Yamaguchi Y, et al. UV-induced DNA damage and melanin content in human skin differing in racial/ethnic origin. Faseb Journal. 2003; 17(6):1177–9. [PubMed: 12692083]
7. Lavker RM, Gerberick GF, Veres D, Irwin CJ, Kaidbey KH. Cumulative effects from repeated exposures to suberythemal doses of UVB and UVA in human skin. Journal of the American Academy of Dermatology. 1995; 32(1):53–62. [PubMed: 7822517]
8. Joseph JM, Destaillats H, Hung HM, Hoffmann MR. The sonochemical degradation of azobenzene and related azo dyes: Rate enhancements via Fenton's reactions. Journal of Physical Chemistry A. 2000; 104(2):301–7.
9. Anderson RR, Parrish JA. The optics of human-skin. Journal of Investigative Dermatology. 1981; 77(1):13–9. [PubMed: 7252245]
10. Philip R, Penzkofer A, Baumler W, Szeimies RM, Abels C. Absorption and fluorescence spectroscopic investigation of indocyanine green. Journal of Photochemistry and Photobiology A: Chemistry. 1996; 96(1-3):137–48.
11. Mohr H, Bachmann B, KleinStruckmeier A, Lambrecht B. Virus inactivation of blood products by phenothiazine dyes and light. Photochemistry and Photobiology. 1997; 65(3):441–5. [PubMed: 9077128]
12. Williamson LM, Cardigan R, Prowse CV. Methylene blue-treated fresh-frozen plasma: what is its contribution to blood safety? Transfusion. 2003; 43(9):1322–9. [PubMed: 12919437]
13. Guyton, A.; Hall, J. Textbook of Medical Physiology. Philidelphia: Elsevier; 2006.
14. Oster G, Holmstrom B, Bellin JS. Photochemistry of riboflavin. Experientia. 1962; 18(6):249–53. [PubMed: 14482582]
15. Vanderputten WJM, Kelly JM. Laser flash spectroscopy of methylene-blue with nucleic-acids - Effects of ionic-strength and pH. Photochemistry and Photobiology. 1989; 49(2):145–51. [PubMed: 2710824]
16. Zhang XZ, Zhuo RX, Yang YY. Using mixed solvent to synthesize temperature sensitive poly(N-isopropylacrylamide) gel with rapid dynamics properties. Biomaterials. 2002; 23(5):1313–8. [PubMed: 11804287]
17. Kim S-H, Chu C-C. Visible light induced dextran-methacrylate hydrogel formation using (-)-riboflavin vitamin B2 as a photoinitiator and L-arginine as a co-initiator. Fibers and Polymers. 2009; 10(1):14–20.
18. Bertolotti SG, Previtali CM, Rufs AM, Encinas MV. Riboflavin triethanolamine as photoinitiator system of vinyl polymerization. A mechanistic study by laser flash photolysis. Macromolecules. 1999; 32(9):2920–4.
19. Floyd RA, Schneider JE, Dittmer DR. Methylene blue photoinactivation of RNA viruses. Antiviral Research. 2004; 61(3):141–51. [PubMed: 15168794]

20. Kim TH, Chen YP, Mount CW, Gombotz WR, Li XD, Pun SH. Evaluation of Temperature-Sensitive, Indocyanine Green-Encapsulating Micelles for Noninvasive Near-Infrared Tumor Imaging. Pharmaceutical Research. 2010; 27(9):1900–13. [PubMed: 20568000]
21. Rao J, Dragulescu-Andrasi A, Yao H. Fluorescence imaging in vivo: recent advances. Current Opinion in Biotechnology. 2007; 18(1):17–25. [PubMed: 17234399]
22. Ntziachristos V, Yodh AG, Schnall M, Chance B. Concurrent MRI and diffuse optical tomography of breast after indocyanine green enhancement. Proceedings of the National Academy of Sciences of the United States of America. 2000; 97(6):2767–72. [PubMed: 10706610]
23. Patel RH, Wadajkar AS, Patel NL, Kavuri VC, Nguyen KT, Liu HL. Multifunctionality of indocyanine green-loaded biodegradable nanoparticles for enhanced optical imaging and hyperthermia intervention of cancer. Journal of Biomedical Optics. 2012; 17(4):10.
24. Dewhirst MW, Viglianti BL, Lora-Michiels M, Hanson M, Hoopes PJ. Basic principles of thermal dosimetry and thermal thresholds for tissue damage from hyperthermia. International Journal of Hyperthermia. 2003; 19(3):267–94. [PubMed: 12745972]
25. Roemer RB. Engineering aspects of hyperthermia therapy. Annual Review of Biomedical Engineering. 1999; 1:347–76.
26. Weissleder R. A clearer vision for in vivo imaging. Nature Biotechnology. 2001; 19(4):316–7.
27. Curcio JA, Petty CC. The Near Infrared Absorption Spectrum of Liquid Water. Journal of the Optical Society of America. 1951; 41(5):302.
28. Tonnessen BH, Pounds L. Radiation physics. Journal of Vascular Surgery. 2011; 53:6S–8S. [PubMed: 20869192]
29. Bergmann K, Okonski CT. A spectroscopic study of methylene blue monomer, dimer, and complexes with montmorillonite. Journal of Physical Chemistry. 1963; 67(10):2169–77.
30. Liebel F, Kaur S, Ruvolo E, Kollias N, Southall MD. Irradiation of Skin with Visible Light Induces Reactive Oxygen Species and Matrix-Degrading Enzymes. Journal of Investigative Dermatology. 2012; 132(7):1901–7. [PubMed: 22318388]
31. Holzer W, Mauerer M, Penzkofer A, Szeimies RM, Abels C, Landthaler M, et al. Photostability and thermal stability of indocyanine green. Journal of Photochemistry and Photobiology B-Biology. 1998; 47(2-3):155–64.
32. Landsman MLJ, Kwant G, Mook GA, Zijlstra WG. Light-absorbing properties, stability, and spectral stabilization of indocyanine green. Journal of Applied Physiology. 1976; 40(4):575–83. [PubMed: 776922]
33. Tardivo JP, Del Giglio A, de Oliveira CS, Gabrielli DS, Junqueira HC, Tada DB, et al. Methylene blue in photodynamic therapy: From basic mechanisms to clinical applications. Photodiagnosis and Photodynamic Therapy. 2005; 2(3):175–91. [PubMed: 25048768]
34. Islam SDM, Penzkofer A, Hegemann P. Quantum yield of triplet formation of riboflavin in aqueous solution and of flavin mononucleotide bound to the LOV1 domain of Phot1 from Chlamydomonas reinhardtii. Chemical Physics. 2003; 291(1):97–114.
35. Ahmad I, Fasihullah Q, Noor A, Ansari IA, Ali QNM. Photolysis of riboflavin in aqueous solution: a kinetic study. International Journal of Pharmaceutics. 2004; 280(1-2):199–208. [PubMed: 15265559]
36. Ahmad I, Sheraz MA, Ahmed S, Kazi SH, Mirza T, Aminuddin M. Stabilizing effect of citrate buffer on the photolysis of riboflavin in aqueous solution. Results in Pharma Sciences. 2011; 1(1): 11–5. [PubMed: 25755977]
37. Chen R, Wang X, Yao XK, Zheng XC, Wang J, Jiang XQ. Near-IR-triggered photothermal/photodynamic dual-modality therapy system via chitosan hybrid nanospheres. Biomaterials. 2013; 34(33):8314–22. [PubMed: 23896004]
38. Hu J, Hou Y, Park H, Choi B, Hou S, Chung A, et al. Visible light crosslinkable chitosan hydrogels for tissue engineering. Acta Biomaterialia. 2012; 8(5):1730–8. [PubMed: 22330279]
39. Grzelak A, Rychlik B, Baptosz G. Light-dependent generation of reactive oxygen species in cell culture media. Free Radical Biology and Medicine. 2001; 30(12):1418–25. [PubMed: 11390187]
40. Varma SD, Kumar S, Richards RD. Light-induced damage to ocular lens cation pump: prevention by vitamin C. Proceedings of the National Academy of Sciences. 1979; 76(7):3504–6.

41. Hah HJ, Kim G, Lee Y-EK, Orringer DA, Sagher O, Philbert MA, et al. Methylene Blue-Conjugated Hydrogel Nanoparticles and Tumor-Cell Targeted Photodynamic Therapy. Macromolecular Bioscience. 2011; 11(1):90–9. [PubMed: 20976722]

42. Phelps MA, Foraker AB, Gao W, Dalton JT, Swaan PW. A Novel Rhodamine–Riboflavin Conjugate Probe Exhibits Distinct Fluorescence Resonance Energy Transfer that Enables Riboflavin Trafficking and Subcellular Localization Studies. Molecular Pharmaceutics. 2004; 1(4): 257–66. [PubMed: 15981585]

43. Gutowska A, Bark JS, Kwon IC, Bae YH, Cha Y, Kim SW. Squeezing hydrogels for controlled oral drug delivery. Journal of Controlled Release. 1997; 48(2-3):141–8.

44. Yoshida R, Sakai K, Okano T, Sakurai Y. Drug release profiles in the shrinking process of thermoresponsive poly(N-isopropylacrylamide-co-alkyl methacrylate) gels. Industrial & Engineering Chemistry Research. 1992; 31(10):2339–45.

45. Alkilany AM, Murphy CJ. Toxicity and cellular uptake of gold nanoparticles: what we have learned so far? Journal of Nanoparticle Research. 2010; 12(7):2313–33. [PubMed: 21170131]

46. Cho W-S, Cho M, Jeong J, Choi M, Cho H-Y, Han BS, et al. Acute toxicity and pharmacokinetics of 13 nm-sized PEG-coated gold nanoparticles. Toxicology and Applied Pharmacology. 2009; 236(1):16–24. [PubMed: 19162059]

47. Viger ML, Sheng W, Dore K, Alhasan AH, Carling C-J, Lux J, et al. Near-Infrared-Induced Heating of Confined Water in Polymeric Particles for Efficient Payload Release. Acs Nano. 2014; 8(5):4815–26. [PubMed: 24717072]

48. Malonne H, Eeckman F, Fontaine D, Otto A, De Vos L, Moes A, et al. Preparation of poly (N-isopropylacrylamide) copolymers and preliminary assessment of their acute and subacute toxicity in mice. European Journal of Pharmaceutics and Biopharmaceutics. 2005; 61(3):188–94. [PubMed: 16006108]

49. Pan Y, Bao H, Sahoo NG, Wu T, Li L. Water-Soluble Poly(N-isopropylacrylamide)-Graphene Sheets Synthesized via Click Chemistry for Drug Delivery. Advanced Functional Materials. 2011; 21(14):2754–63.

50. Patenaude M, Hoare T. Injectable, Degradable Thermoresponsive Poly(N-isopropylacrylamide) Hydrogels. Acs Macro Letters. 2012; 1(3):409–13.

51. Vihola H, Laukkanen A, Valtola L, Tenhu H, Hirvonen J. Cytotoxicity of thermosensitive polymers poly(N-isopropylacrylamide), poly(N-vinylcaprolactam) and amphiphilically modified poly(N-vinylcaprolactam). Biomaterials. 2005; 26(16):3055–64. [PubMed: 15603800]

52. Wadajkar AS, Koppolu B, Rahimi M, Nguyen KT. Cytotoxic evaluation of N-isopropylacrylamide monomers and temperature-sensitive poly(N-isopropylacrylamide) nanoparticles. Journal of Nanoparticle Research. 2009; 11(6):1375–82.

53. Park SH, Choi BG, Moon HJ, Cho S-H, Jeong B. Block sequence affects thermosensitivity and nano-assembly: PEG-L-PA-DL-PA and PEG-DL-PA-L-PA block copolymers. Soft Matter. 2011; 7(14):6515–21.

54. Park MH, Joo MK, Choi BG, Jeong B. Biodegradable Thermogels. Accounts of Chemical Research. 2012; 45(3):424–33. [PubMed: 21992012]

55. Lee S-M, Park H, Yoo K-H. Synergistic Cancer Therapeutic Effects of Locally Delivered Drug and Heat Using Multifunctional Nanoparticles. Advanced Materials. 2010; 22(36):4049–53. [PubMed: 20665571]

56. Xiao Z, Ji C, Shi J, Pridgen EM, Frieder J, Wu J, et al. DNA Self-Assembly of Targeted Near-Infrared-Responsive Gold Nanoparticles for Cancer Thermo-Chemotherapy. Angewandte Chemie-International Edition. 2012; 51(47):11853–7.

57. Shiotani A, Mori T, Niidome T, Niidome Y, Katayama Y. Stable incorporation of gold nanorods into N-isopropylacrylamide hydrogels and their rapid shrinkage induced by near-infrared laser irradiation. Langmuir. 2007; 23(7):4012–8. [PubMed: 17311430]

58. Dong K, Liu Z, Li Z, Ren J, Qu X. Hydrophobic Anticancer Drug Delivery by a 980 nm Laser-Driven Photothermal Vehicle for Efficient Synergistic Therapy of Cancer Cells In Vivo. Advanced Materials. 2013; 25(32):4452–8. [PubMed: 23798450]

59. Jayakumar MKG, Idris NM, Zhang Y. Remote activation of biomolecules in deep tissues using near-infrared-to-UV upconversion nanotransducers. Proceedings of the National Academy of Sciences of the United States of America. 2012; 109(22):8483–8. [PubMed: 22582171]

60. Carter KA, Shao S, Hoopes MI, Luo D, Ahsan B, Grigoryants VM, et al. Porphyrin-phospholipid liposomes permeabilized by near-infrared light. Nature Communications. 2014; 5:1–11.

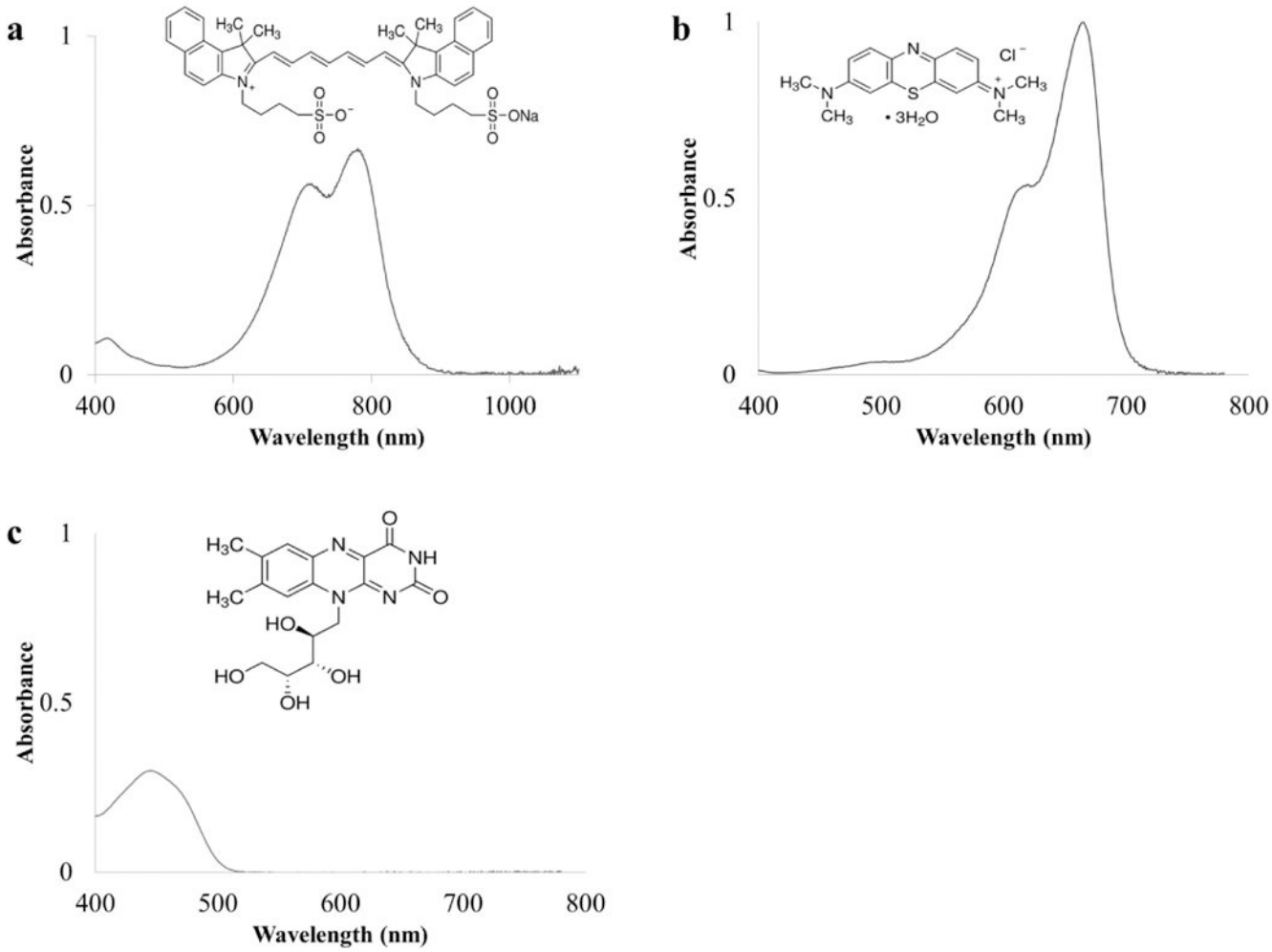

Fig. 1.

The absorbance spectra and chemical structures of (a) cardiogreen (13μM), (b) methylene blue (16μM), and (c) riboflavin (26μM) in water.

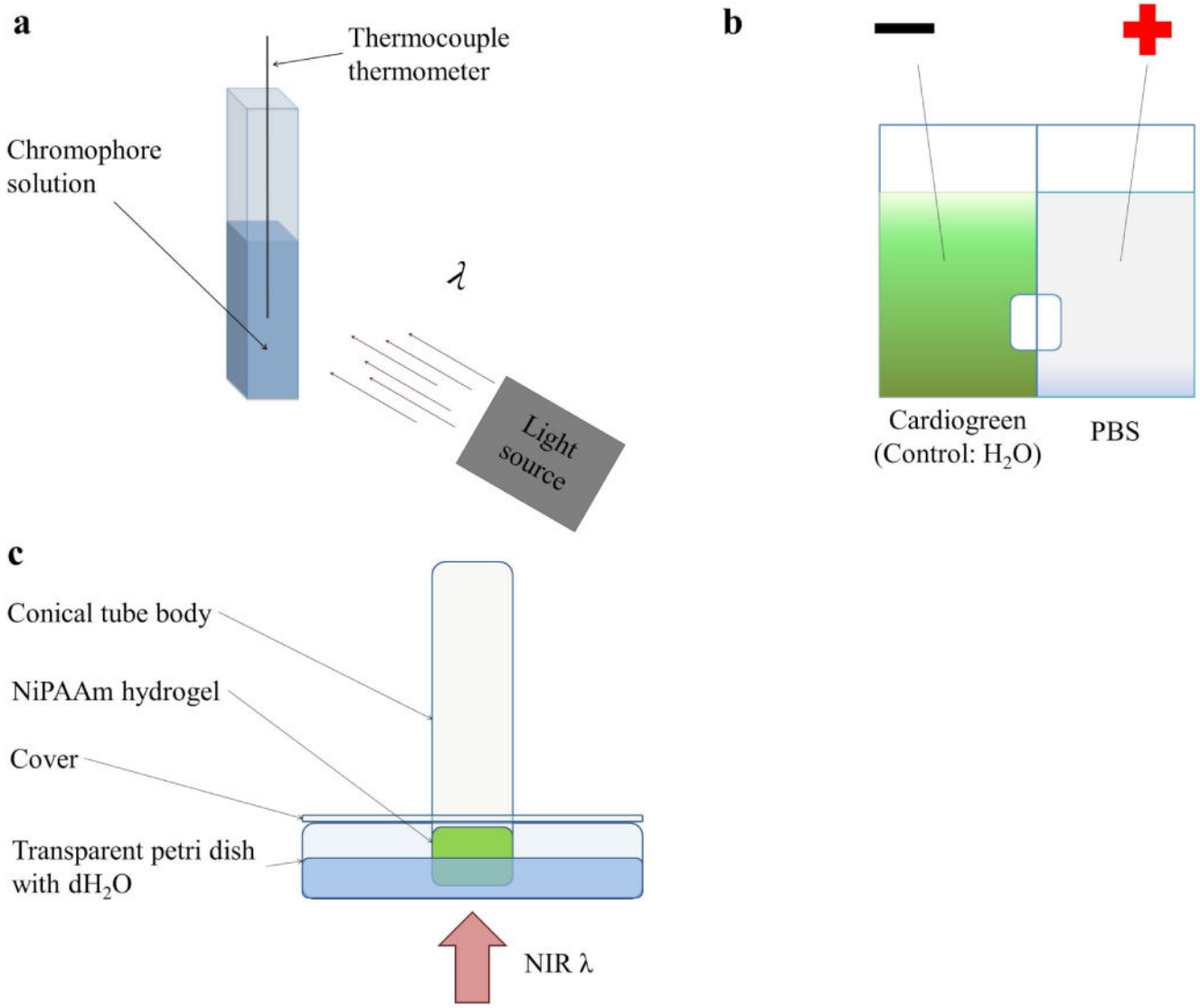

Fig. 2.

Illustrations of the experimental setup for (a) irradiating aqueous solutions of each chromophore with visible and NIR light; (b) loading cardiogreen into NiPAAm hydrogels via electrophoresis; and (c) measuring the light actuated of release of BSA from NiPAAm hydrogels.

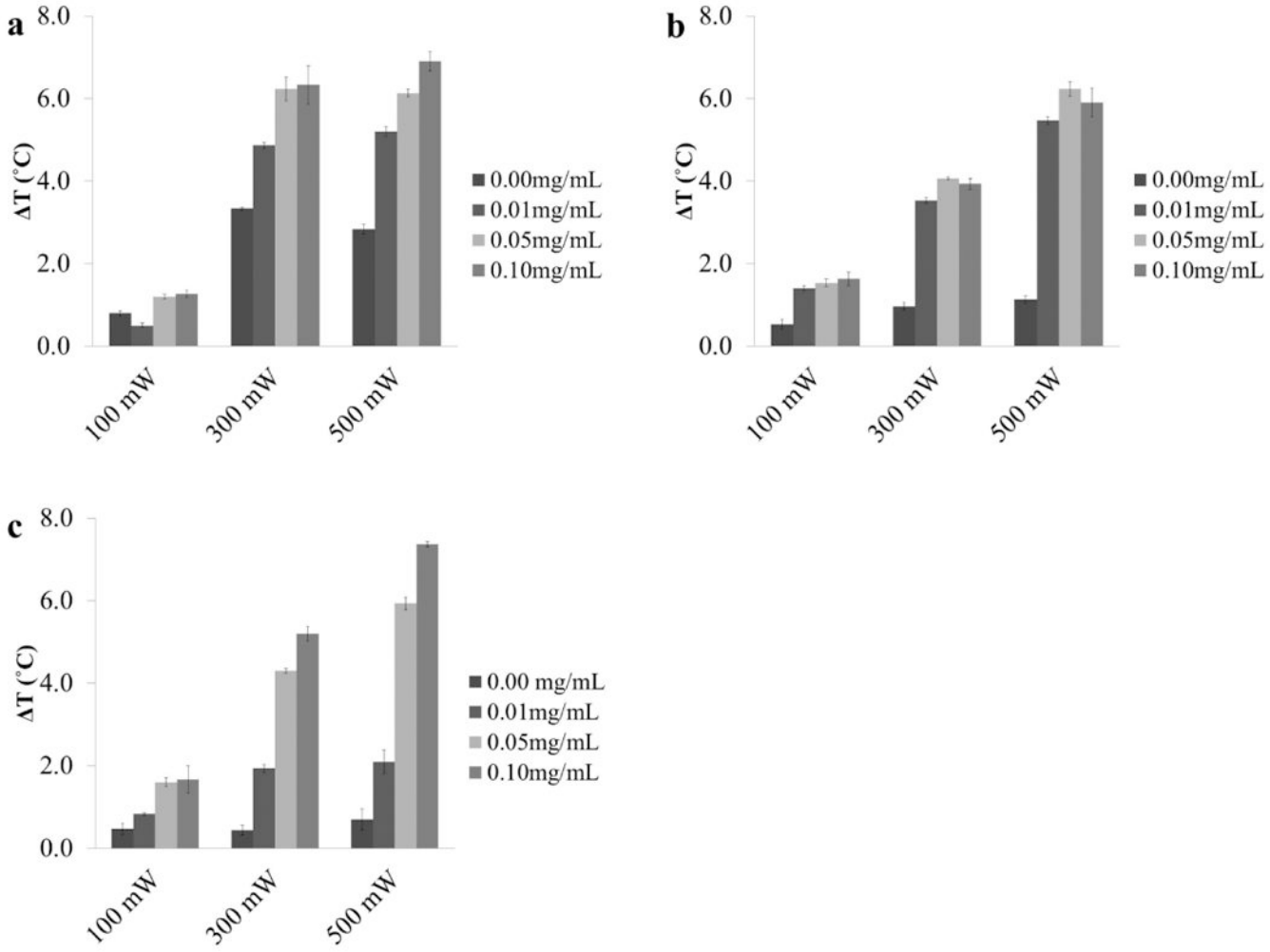

Fig. 3.

The measured temperature change of 1 mL aqueous solutions with 0, 0.01, 0.05, and 0.1mg/mL of (a) cardiogreen, (b) methylene blue and (c) riboflavin after 5 min of light exposure (cardiogreen: 900 nm; methylene blue: 650 nm; and riboflavin: 450 nm) at 100, 300 and 500mW (n=3). For each chromophore studied, increasing the concentration of chromophore, the power of the light source, or both increased the measured temperature changes.

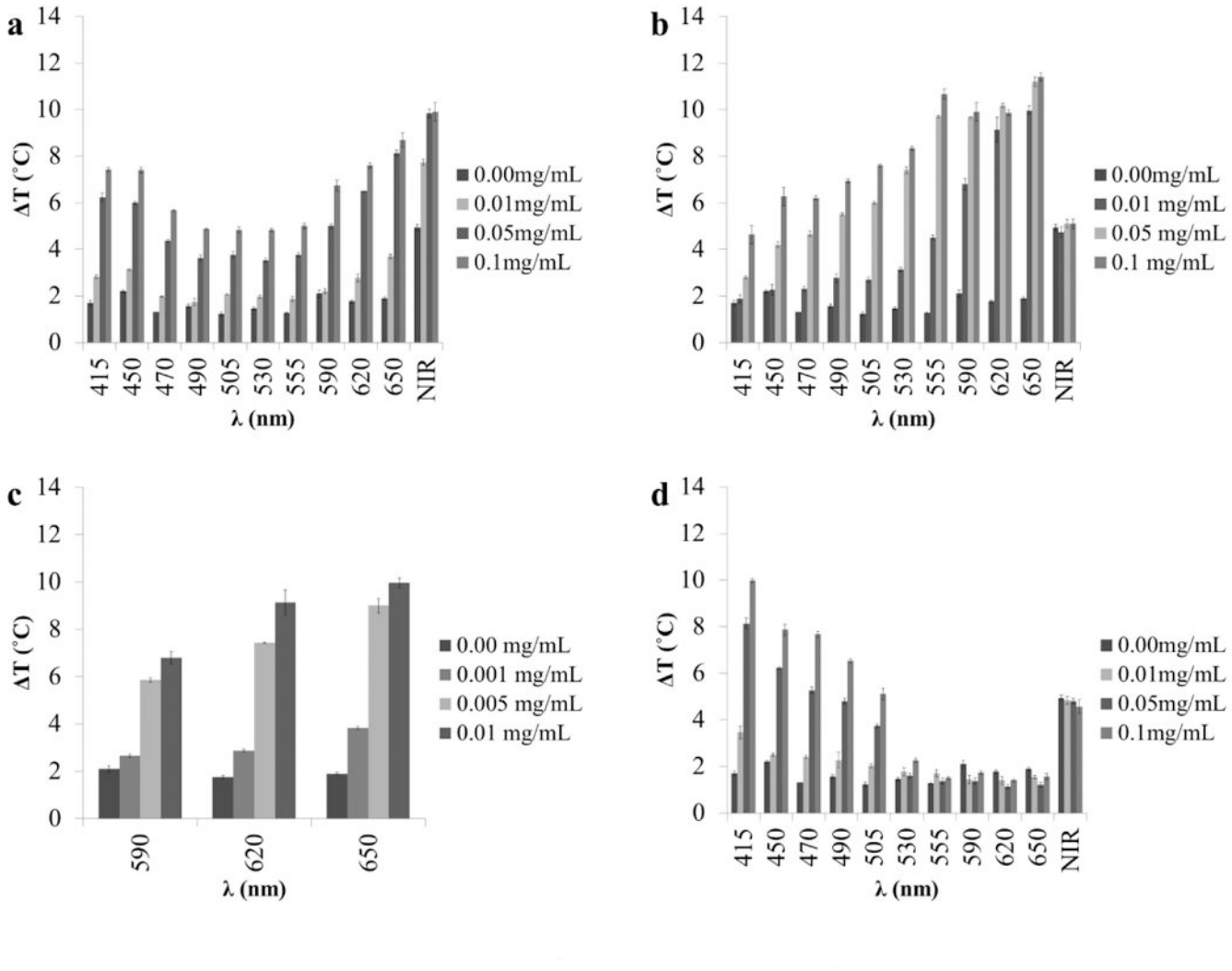

Fig. 4.

The measured temperature change of 1 mL aqueous solutions with varying concentrations of (a) cardiogreen, (b–c) methylene blue, and (d) riboflavin after 5 min of exposure to varying wavelengths of visible and NIR light at 600mW (n=3). Chromophores show a wavelength dependent change in temperature with the greatest temperature change falling within the chromophore's absorption band.

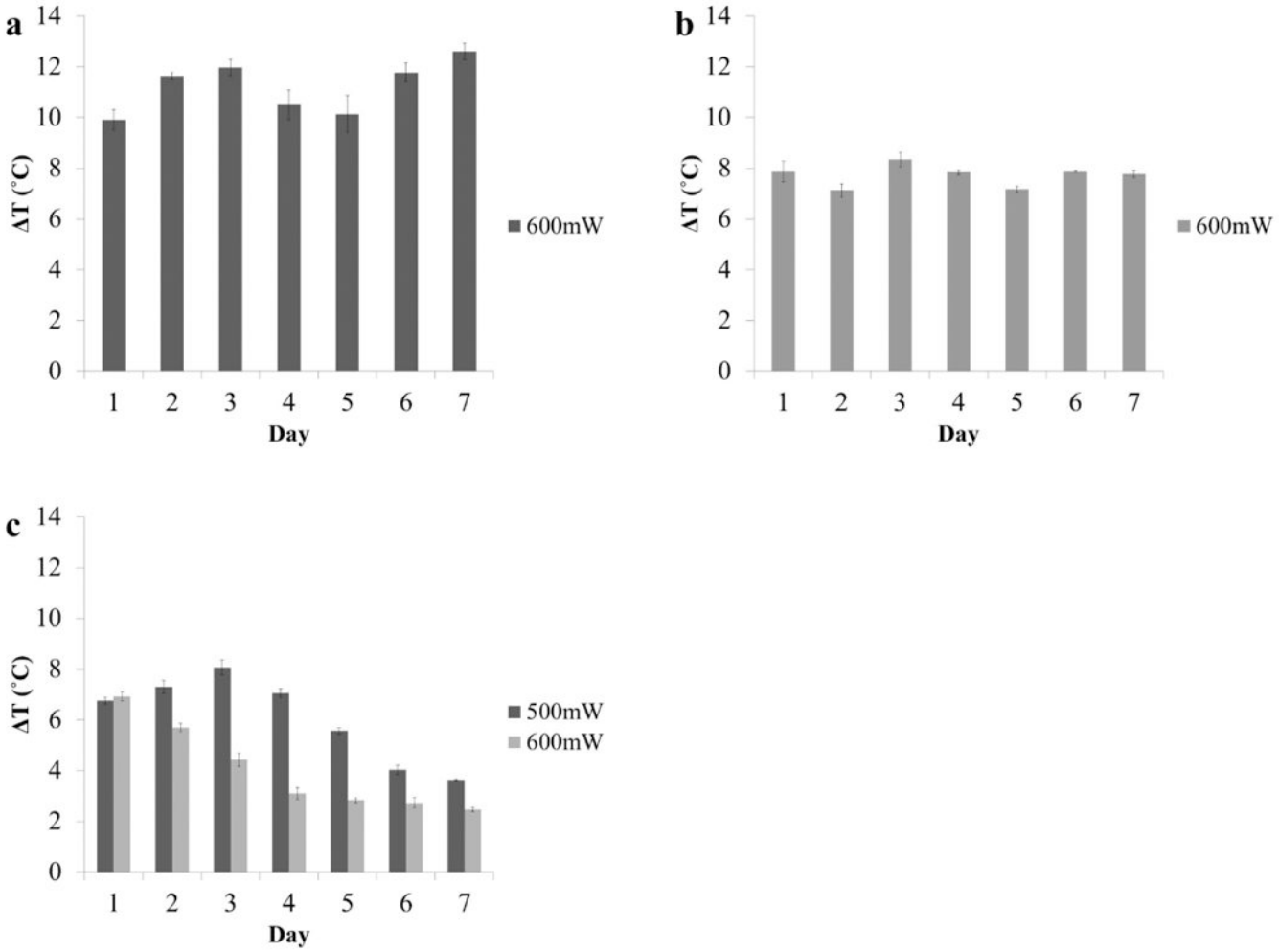

Fig. 5.

The measured temperature change of 1 mL aqueous solutions with 0.1mg/mL of (a) cardiogreen, (b) methylene blue and (c) riboflavin after 5 min of light exposure every day for 7 days (cardiogreen: 900nm; methylene blue: 650nm; and riboflavin: 450nm) at 600mW (n=3). No loss in photothermal response from cardiogreen and methylene blue while the photothermal response steadily decreases for riboflavin after the first exposure. Decreasing the light power to 500mW prolongs the photothermal response but begins to decrease after the third exposure at day 3.

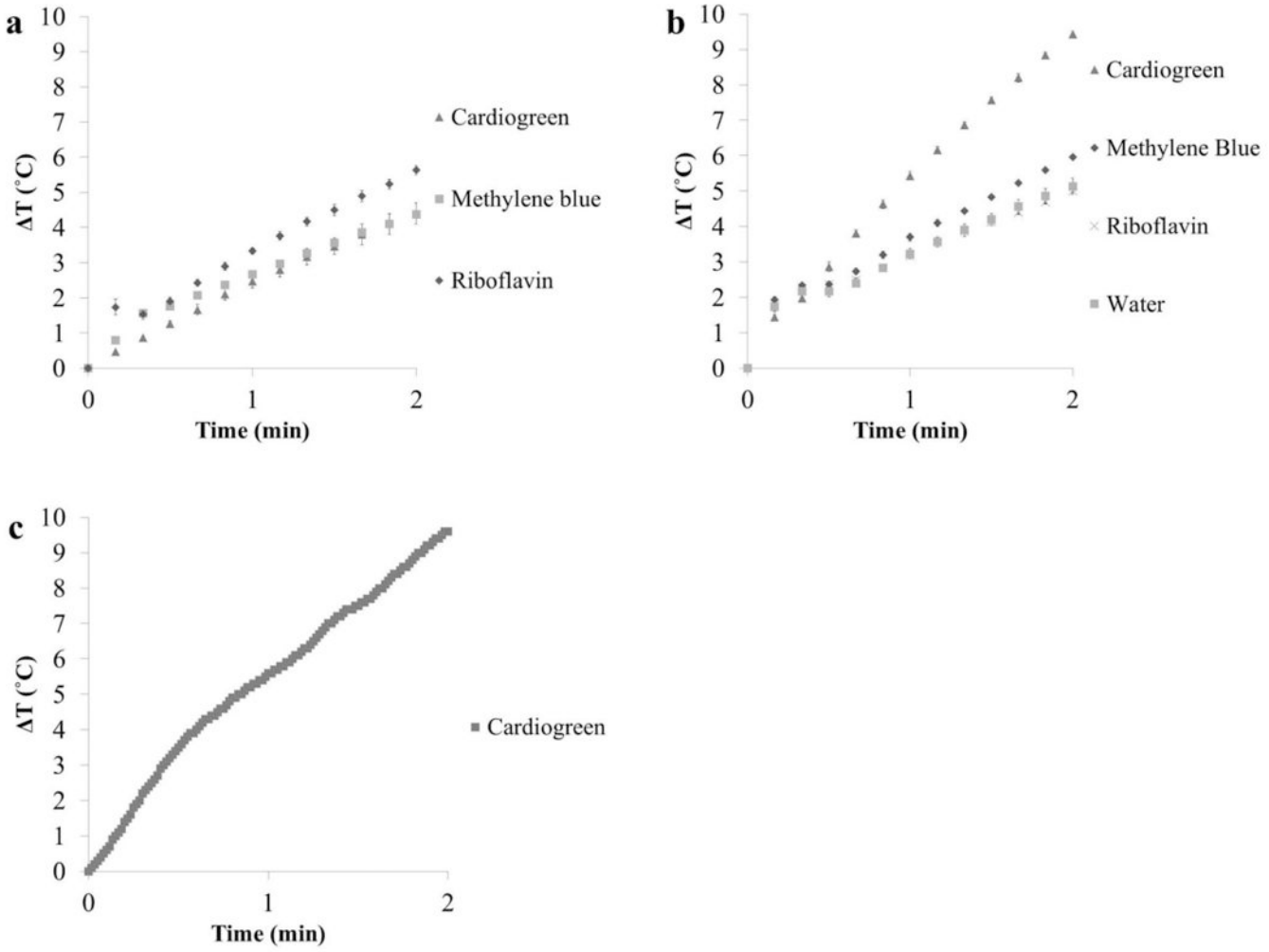

Fig. 6.

Comparing the rate of temperature change from 0.1mg/mL solutions of cardiogreen, methylene blue and riboflavin exposed to (a) 600mW of light (450 nm for riboflavin, 650 nm for methylene blue, and 715 nm for cardiogreen) (volume = 1mL), and (b) 750mW of NIR light (715 nm, bandwidth = 30 nm) (volume = 500μL) (n=3). (c) The rate of temperature change of a cardiogreen-loaded NiPAAm hydrogel irradiated with 750mW of NIR light. Cardiogreen is loaded into NiPAAm hydrogel via electrophoresis (see Supplement Fig. 1 for amount of cardiogreen loaded).

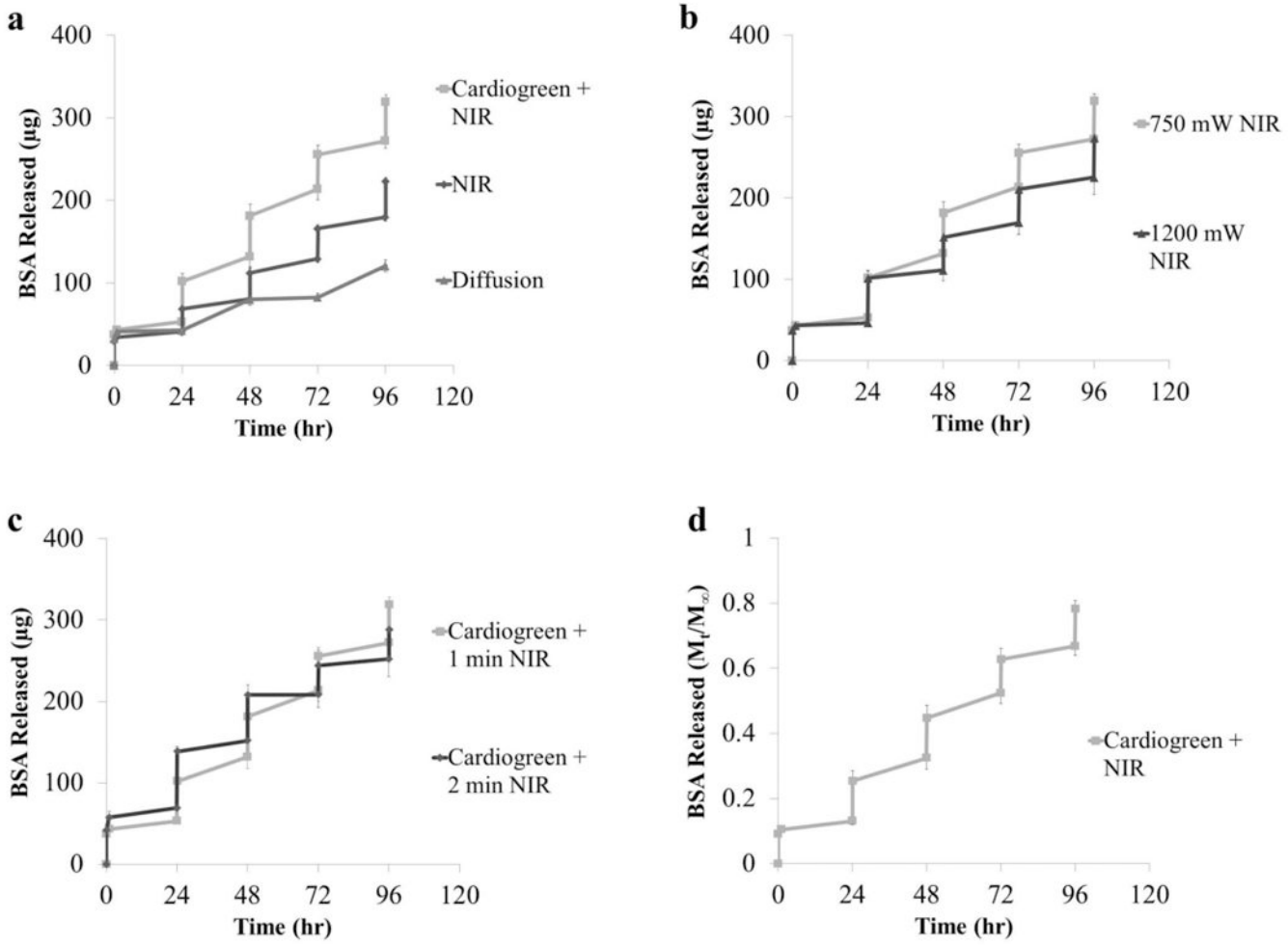

Fig. 7.

The cumulative release (µg, a-c) and percent release (d) of BSA (66kDa) from NiPAAm hydrogels (diameter = 9mm, thickness = 4mm) via the photothermal response of cardiogreen irradiated with NIR light. Irradiation occurred every 24 h starting at t=24hr. (a) Comparing the triggered release versus diffusion of BSA from NiPAAm hydrogels (n=4). 'Cardiogreen + NIR' and 'NIR' samples were irradiated with 750mW NIR light for 1 minute. (b) Comparing the BSA release from cardiogreen-loaded NiPAAm hydrogels irradiated with 750mW and 1200mW NIR light for 1 minute (n=4). (c) Comparing the BSA release from cardiogreen-loaded NiPAAm hydrogels irradiated with 750mW NIR light for 1 and 2 min (n=4). (d) The percent release of BSA from cardiogreen-loaded NiPAAm hydrogels irradiated with 750mW NIR light for 1 minute. M_t is cumulative release at time, t, and M_∞ is cumulative release after 14 days (n=4).

Table 1
Summary of chromophore properties and photothermal response

Chromophore	Riboflavin	Methylene Blue	Cardiogreen
Molecular weight	376.36 g/mol	319.85 g/mol	774.96 g/mol
λ_{abs} max.	445 nm	665 nm	775 nm
Quantum efficiency for fluorescence	0.25	0.04	0.19
Solubility in H_2O	84.7 mg/L	4.36×10^4 mg/L	1×10^3 mg/L
Max. ΔT after 2 min. exposure at 600mW; C = 0.1 mg/mL; (λ)	5.6°C (450 nm)	4.3°C (650 nm)	5.5°C (780 nm)
ΔT of H_2O after 2 min. exposure at 600mW (λ)	1.2°C (450 nm)	1.9°C (650 nm)	3.2°C (780 nm)

Table 2

Summary of select near infrared light actuated delivery-on-demand systems compared to reported system

Wavelength	Power	Time	Chromophore	Outcome	Ref.
808 nm (CW diode laser)	2.56W/cm^2	10 min	PEG-PLGA-Au half-shell nanoparticles (120 nm diameter)	0.25 mg/kg DOX released 24 h post-injection by NIR irradiation. DOX persisted for 72 h in tumor	[55]
808 nm (CW diode laser)	600mW	5, 10 min	Gold nanorods (50 × 10 nm)	All DOX released with 10 min exposure. Very little at 5 min. despite ΔT = 40°C within 1 min.	[56]
1064nm (Nd:YVO_4 laser)	750mW	30 s	Gold nanorods (65 × 11 nm)	Rapid release of rhodamine-labeled dextran from NiPAAm hydrogels (d = 140 μm)	[57]
980 nm (NIR laser)	0.7W/cm^2	20 min	Hallow CuS nanoparticles (0.1 mg/mL)	60% of camptothecin released after 3× 20 min (4.5% to 18.8% bursts) NIR light exposures over 80 h.	[58]
980 nm (CW NIR laser)	2.8W/cm^2	12 min	NIR-to-UV upconversion nanoparticles	siRNA for GFP photocaged by 4,5-dimethoxy-2-nitroacetophenone significantly decreased GFP fluorescence intensity 32 h post-exposure to NIR	[59]
980 nm (CW diode laser)	1W	5 min	water	70% release of fluorescein after 5× 5 min NIR light exposures from PLGA delivery vehicle (size =0.5 μm; T_g = 42°C) over 90 min.	[47]
658 nm (laser)	300mW	4 min	(HPPH)-lipids	Minimal release of DOX for 2 days when soaked in 10% serum; 100 % release of DOX after 4 min of exposure to NIR light.	[60]
900 nm (non-coherent light)	750mW	1 min	cardiogreen	80% of BSA released from NiPAAm after 4× 1 min (11-12% bursts) NIR light exposures over 96 h (4 days).	

Acronyms: continuous wave, CW; polyethylene glycol, PEG; poly (lactic-co-glycolic acid), PLGA; doxorubicin, DOX; near infrared, NIR; poly (N-isopropylacrylamide), NiPAAm; ultraviolet, UV; small interfering ribonucleic acid, siRNA; green fluorescent protein, GFP; devinyl hexyloxyethy-pyropheophorbide, HPPH; bovine serum albumin, BSA.